Quantum Inf Process (2016) 15:2685–2700
DOI 10.1007/s11128-016-1318-8

# Quantum image coding with a reference-frame-independent scheme

**François Chapeau-Blondeau**[1] · **Etienne Belin**[1]

Received: 28 September 2015 / Accepted: 6 April 2016 / Published online: 23 April 2016


**Abstract** For binary images, or bit planes of non-binary images, we investigate the possibility of a quantum coding decodable by a receiver in the absence of reference frames shared with the emitter. Direct image coding with one qubit per pixel and non-aligned frames leads to decoding errors equivalent to a quantum bit-flip noise increasing with the misalignment. We show the feasibility of frame-invariant coding by using for each pixel a qubit pair prepared in one of two controlled entangled states. With just one common axis shared between the emitter and receiver, exact decoding for each pixel can be obtained by means of two two-outcome projective measurements operating separately on each qubit of the pair. With strictly no alignment information between the emitter and receiver, exact decoding can be obtained by means of a two-outcome projective measurement operating jointly on the qubit pair. In addition, the frame-invariant coding is shown much more resistant to quantum bit-flip noise compared to the direct non-invariant coding. For a cost per pixel of two (entangled) qubits instead of one, complete frame-invariant image coding and enhanced noise resistance are thus obtained.

**Keywords** Quantum image processing · Quantum image coding · Entangled qubits · Quantum noise · Mutual information

✉ François Chapeau-Blondeau
chapeau@univ-angers.fr

Etienne Belin
etienne.belin@univ-angers.fr

[1] Laboratoire Angevin de Recherche en Ingénierie des Systèmes (LARIS), Université d'Angers, 62 avenue Notre Dame du Lac, 49000 Angers, France

## 1 Introduction

Quantum representation or coding becomes a natural requirement for images when their storage or communication is envisaged at the level of individual elementary constituents, like photons, electrons, atoms or nanodevices, as implied by the progress of information technologies. In addition, under a quantum form, images get access to the powerful potentialities of quantum computation and quantum algorithms for information processing. A quantum variant of digital image processing is, however, still in a very early stage of elaboration [1]. To begin with, the basic issue of coding an image under a quantum form can be approached in several different ways, as, for instance, witnessed in the studies of [2–10] and the very recent survey [11], depending on the aims and targeted properties. Here we shall examine a property not previously addressed for quantum images, and dealing with possible forms of quantum coding enabling invariance or independence with respect to the reference frame used for quantum measurement and decoding.

Quantum measurement typically is referred to a given projective basis. Changing the measurement basis usually changes the measurement outcomes and their statistics. For storage, retrieval, communication of information between an emitter and a receiver, aligned reference frames are usually presumed, in order to enable actual transmission of information in a controlled way [12]. This implicitly requires that some prior alignment information be established with the emitter, before the receiver can start to perform quantum measurement with interpretable outcomes [12]. This requirement is sometimes very stringent in practice. To circumvent this limitation, different schemes have been proposed so as to obtain frame independence for various quantum information tasks of interest, such as cryptographic key distribution [13], non-local correlation establishment [14] or entanglement assertion [15–17]. Here, we address frame independence for quantum image coding.

## 2 Single-qubit pixel coding

Our starting point is a standard classical digital image, for which we envisage a quantum coding where each pixel of the image will be represented (coded) by a quantum system prepared in some controlled state. This can be motivated, for instance, by the storage or communication of the image with quantum technologies, to benefit from very high density storage or communication capacity at a quantum level. As is very often the case with digital images, we will consider that the coding of the spatial locations of the pixels is implicit and experiences no other coding. It is ensured, for instance, by the temporal sequence of the stream of quantum states supporting the image in a communication process, or by the spatial location of the physical systems materializing the quantum states in a solid-state storage, or by the logical structure of sequential addressing of a memory. So we will only consider quantum coding of the pixel values or intensities.

A possible quantum coding of an image consists in assigning to each pixel a qubit prepared in a pure state of the form

$$|\psi\rangle = \alpha_0 |0\rangle + \alpha_1 |1\rangle , \tag{1}$$

with $\{|0\rangle , |1\rangle\}$ an orthonormal basis of the complex two-dimensional Hilbert space $\mathcal{H}_2$, and $\alpha_0$ and $\alpha_1$ two complex numbers satisfying the normalization condition $|\alpha_0|^2 + |\alpha_1|^2 = 1$. From the quantum-coded image, through quantum measurement, one then wants to be able recover the original classical image. When the qubit in state $|\psi\rangle$ is measured via a projective measurement in the computational basis $\{|0\rangle , |1\rangle\}$, according to the Born rule, the probability of projecting on $|0\rangle$ is $|\alpha_0|^2 = |\langle 0|\psi\rangle|^2$ while the probability of projecting on $|1\rangle$ is $|\alpha_1|^2 = |\langle 1|\psi\rangle|^2 = 1 - |\alpha_0|^2$. In this way, the result of the quantum measurement of an image is intrinsically random. One can assign to the recovered pixel a value 0 when projecting on $|0\rangle$, and a value 1 when projecting on $|1\rangle$. Over repeated measurements on a large number of copies with the same preparation $|\psi\rangle$, the average value for the pixel is obtained as $|\alpha_1|^2 = 1 - |\alpha_0|^2$. This provides the ability to encode an arbitrary intensity or gray level $|\alpha_1|^2 \in [0, 1]$ for each pixel of the image [3,5–7]. In this form of quantum coding, the intensity of each pixel is coded via the coordinate $\alpha_1$ in the qubit state of Eq. (1). To recover the classical image via quantum measurement requires averaging over a large number of identical copies of the array of qubits materializing the quantum code. This statistical approach, however, enables the recovery of a classical image with an arbitrary distribution of gray levels over [0, 1].

Another possible form of quantum coding considers binary images, as in [10] for instance. A binary image with pixel values at 0 or 1 can also be seen as one bit plane of a gray-level image, with typically 8 such bit planes to represent an image with each gray level coded with a byte of data. For such a binary image, a natural quantum coding is to assign to each pixel a qubit, with for a pixel at 0 the qubit state $|0\rangle$ and for a pixel at 1 the qubit state $|1\rangle$. In this way, measuring a single copy of each qubit of the two-dimensional array, via a projective measurement in the computational orthonormal basis $\{|0\rangle , |1\rangle\}$, enables deterministic recovery of the classical binary image.

This mode of quantum coding of binary images avoids the requirement of a statistical recovery via an average over a series of measurements on a large number of identical copies needed for a gray-level image. Instead, from measurement of a single quantum image, it enables deterministic recovery of the classical binary image. There is, however, a limitation with such deterministic recovery of a binary image. Each qubit, which is prepared either in state $|0\rangle$ or in state $|1\rangle$ at each pixel, need be measured precisely in the original coding basis $\{|0\rangle , |1\rangle\}$ for a correct deterministic recovery of the classical binary information. This requires the emitter performing quantum coding of the image, and the receiver performing the decoding, to share a common reference frame, and this may sometimes represent a stringent condition.

Suppose the receiver, instead of measuring in the original (coding) orthonormal basis $\{|0\rangle , |1\rangle\}$, measures in an orthonormal basis $\{|0'\rangle , |1'\rangle\}$ rotated by an angle $\xi$ according to

$$\begin{cases} |0'\rangle = +\cos(\xi) |0\rangle + \sin(\xi) |1\rangle , \\ |1'\rangle = -\sin(\xi) |0\rangle + \cos(\xi) |1\rangle , \end{cases} \tag{2}$$

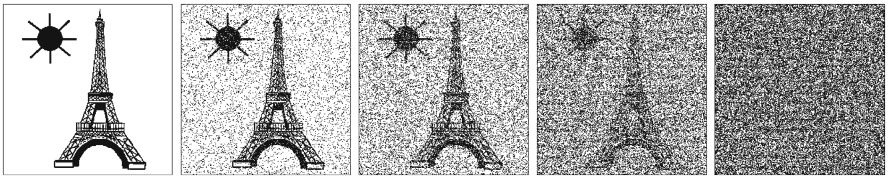

**Fig. 1** A $256 \times 256$ pixel binary image coded for each pixel with a qubit in state $|0\rangle$ or $|1\rangle$, and decoded by measuring the qubit in the basis $\{|0'\rangle, |1'\rangle\}$ of Eq. (2) rotated by the angle $\xi$ relative to the coding basis $\{|0\rangle, |1\rangle\}$, with from *left* to *right* $\xi = 0, 0.1\pi, 0.15\pi, 0.2\pi$ and $0.25\pi$

equivalent to the inverse relation

$$\begin{cases} |0\rangle = \cos(\xi)\,|0'\rangle - \sin(\xi)\,|1'\rangle\,, \\ |1\rangle = \sin(\xi)\,|0'\rangle + \cos(\xi)\,|1'\rangle\,, \end{cases} \tag{3}$$

and both Eqs. (2) and (3) will be useful for expressing the points of view of the decoding and of the coding stages. When measuring in the rotated basis $\{|0'\rangle, |1'\rangle\}$, the receiver decodes the pixel value 0 when the measurement projects on $|0'\rangle$, and it decodes the pixel value 1 when the measurement projects on $|1'\rangle$. In this way, when in the basis $\{|0'\rangle, |1'\rangle\}$ measurement is performed on the qubit state $|0\rangle$, the pixel value 0 is decoded with a (conditional) probability given by the squared inner product $\Pr\{0 \,|\, |0\rangle\} = |\langle 0'|0\rangle|^2 = \cos^2(\xi)$; when measurement is performed on the qubit state $|1\rangle$, the pixel value 1 is decoded with probability $\Pr\{1 \,|\, |1\rangle\} = |\langle 1'|1\rangle|^2 = \cos^2(\xi)$. So, when measuring in the basis $\{|0'\rangle, |1'\rangle\}$ of Eq. (2) rotated by the angle $\xi$, each pixel value of the binary image is correctly recovered only with probability $\cos^2(\xi)$, which consistently matches 1 at $\xi = 0$ with no rotation. For a rotation angle $\xi \neq 0$, Fig. 1 illustrates the degradation in the decoding process incurred by measuring the quantum image in the rotated basis $\{|0'\rangle, |1'\rangle\}$ instead of the coding basis $\{|0\rangle, |1\rangle\}$.

In Fig. 1, at the rotation angle $\xi = 0$ no decoding error occurs and the binary image is perfectly restored by the receiver. As the angle $\xi$ increases above zero in Fig. 1, decoding errors occur with a probability $1 - \cos^2(\xi) = \sin^2(\xi)$ at each pixel. As a result, the decoded binary image progressively degrades, as visible in Fig. 1. The degradation increases with $\xi$ up to the angle $\xi = \pi/4$ where degradation is maximal, with a probability of error $\sin^2(\pi/4) = 1/2$ at each pixel, resulting in a completely random binary image decoded by the receiver in Fig. 1. If the angle $\xi$ was further increased from $\pi/4$ to $\pi/2$, then the decoding would start to progressively favor a deterministic inversion of the binary value at each pixel. Ultimately, at $\xi = \pi/2$, the probability of decoding error would be $\sin^2(\pi/2) = 1$, which amounts to a deterministic inversion of each binary pixel, restoring precisely an inverted version of the input binary image, which would preserve the essential constitutive information of the input image. So it is indeed the angle $\xi = \pi/4$ restoring a purely random image as in Fig. 1 which represents the worse condition for decoding.

The mismatch by an angle $\xi$ between the coding and decoding bases, leading to a probability of decoding error of $\sin^2(\xi)$ at each pixel, produces a detrimental effect equivalent to the degradation inflicted by a quantum bit-flip noise acting before a

decoding which would take place with otherwise aligned frames. In general, on a qubit in a state represented by the density operator $\rho$, the action of the bit-flip noise [18] leaves the state $\rho$ unchanged with probability $1 - p$ while it applies the Pauli operator $\sigma_x$ flipping the quantum state with probability $p$. This can be represented by the quantum operation realized by the superoperator $\mathcal{N}(\cdot)$ transforming the qubit state $\rho$ into the qubit state $\mathcal{N}(\rho)$ defined by

$$\mathcal{N}(\rho) = (1 - p)\rho + p\sigma_x \rho \sigma_x^{\dagger}. \tag{4}$$

When a binary image coded in the basis $\{|0\rangle, |1\rangle\}$ is degraded by the bit-flip noise of Eq. (4) with flipping probability $p = \sin^2(\xi)$ prior to the decoding which takes place in the same basis $\{|0\rangle, |1\rangle\}$, the degradation is equivalent to that illustrated in Fig. 1 caused by a mismatch angle $\xi$ between the coding and decoding bases with no noise.

The task of aligning two distant reference frames represents a costly process in terms of transmission and measurement [19]. Alignment methods [12,20–24] are usually based on repeated transmissions and measurements, so as to progressively estimate the frame orientation. In principle, exact estimation of this orientation requires an infinite quantity of information. In practice, alignment is usually performed with a limited precision, entailing some remaining mismatch angle $\xi$, with an impact as exemplified in Fig. 1. The eventuality of time-varying orientations of the reference frames is another feature to complicate the alignment process.

To avoid the detrimental effect of a mismatch between the coding and decoding bases, as illustrated in Fig. 1, and also avoid the costly process of performing frame alignment, the proposal here is to show the feasibility of a frame-independent image coding by exploiting quantum entanglement. Entangled qubit states have stronger invariance properties in a change of basis than single-qubit states. This property will provide the ground for frame-independent image coding.

## 3 Pixel coding by an entangled qubit pair

For a binary image as in Sect. 2, each pixel will be coded by means of a qubit pair of $\mathcal{H}_2 \otimes \mathcal{H}_2$ prepared in one of two controlled entangled states. The pixel value 0 is coded by the state $|\beta_{00}\rangle$, and the pixel value 1 is coded by the state $|\beta_{11}\rangle$, where we refer to the so-called Bell states of an entangled qubit pair expressible from the computational basis $\{|0\rangle, |1\rangle\}$ local to the coding stage as [18]

$$|\beta_{00}\rangle = \frac{1}{\sqrt{2}}\Big(|00\rangle + |11\rangle\Big), \tag{5}$$

$$|\beta_{11}\rangle = \frac{1}{\sqrt{2}}\Big(|01\rangle - |10\rangle\Big). \tag{6}$$

When measuring each qubit by projecting in the basis $\{|0\rangle, |1\rangle\}$, the state $|\beta_{00}\rangle$ always leads to two qubits which are simultaneously found in the same state, either $|0\rangle$ or $|1\rangle$; meanwhile, the state $|\beta_{11}\rangle$ always leads to two qubits which are found in opposite states, either $|0\rangle$ or $|1\rangle$. In this way, when measuring separately the qubits of the pair,

the outcome of two qubits found in the same state decodes the pixel value 0, while the outcome of two qubits in opposite states decodes the pixel value 1. This recovers deterministically, with no error, the encoded pixel value, by separate measurement of two individual qubits in the original basis $\{|0\rangle , |1\rangle\}$.

We now examine how the two coding states $\big(|\beta_{00}\rangle , |\beta_{11}\rangle\big)$ of Eqs. (5)–(6) are seen from the rotated basis $\{|0'\rangle , |1'\rangle\}$ of Eq. (2). From Eq. (3), we have

$$\begin{aligned} |00\rangle &= \big(\cos(\xi)\,|0'\rangle - \sin(\xi)\,|1'\rangle\big) \otimes \big(\cos(\xi)\,|0'\rangle - \sin(\xi)\,|1'\rangle\big), \\ &= \cos^2(\xi)\,|0'0'\rangle + \sin^2(\xi)\,|1'1'\rangle - \cos(\xi)\sin(\xi)\big(|0'1'\rangle + |1'0'\rangle\big). \end{aligned} \tag{7}$$

In a similar way, from Eq. (3),

$$\begin{aligned} |11\rangle &= \big(\sin(\xi)\,|0'\rangle + \cos(\xi)\,|1'\rangle\big) \otimes \big(\sin(\xi)\,|0'\rangle + \cos(\xi)\,|1'\rangle\big), \\ &= \sin^2(\xi)\,|0'0'\rangle + \cos^2(\xi)\,|1'1'\rangle + \cos(\xi)\sin(\xi)\big(|0'1'\rangle + |1'0'\rangle\big). \end{aligned} \tag{8}$$

With Eqs. (7)–(8) substituted in Eq. (5), we therefore obtain

$$|\beta_{00}\rangle = \frac{\cos^2(\xi) + \sin^2(\xi)}{\sqrt{2}}\Big(|0'0'\rangle + |1'1'\rangle\Big) = \frac{1}{\sqrt{2}}\Big(|0'0'\rangle + |1'1'\rangle\Big) = |\beta'_{00}\rangle\,. \tag{9}$$

Also, from Eq. (3) we have

$$\begin{aligned} |01\rangle &= \big(\cos(\xi)\,|0'\rangle - \sin(\xi)\,|1'\rangle\big) \otimes \big(\sin(\xi)\,|0'\rangle + \cos(\xi)\,|1'\rangle\big), \\ &= \cos(\xi)\sin(\xi)\big(|0'0'\rangle - |1'1'\rangle\big) + \cos^2(\xi)\,|0'1'\rangle - \sin^2(\xi)\,|1'0'\rangle\,. \end{aligned} \tag{10}$$

In a similar way, from Eq. (3),

$$\begin{aligned} |10\rangle &= \big(\sin(\xi)\,|0'\rangle + \cos(\xi)\,|1'\rangle\big) \otimes \big(\cos(\xi)\,|0'\rangle - \sin(\xi)\,|1'\rangle\big), \\ &= \cos(\xi)\sin(\xi)\big(|0'0'\rangle - |1'1'\rangle\big) - \sin^2(\xi)\,|0'1'\rangle + \cos^2(\xi)\,|1'0'\rangle\,. \end{aligned} \tag{11}$$

With Eqs. (10)–(11) substituted in Eq. (6), we therefore obtain

$$|\beta_{11}\rangle = \frac{\cos^2(\xi) + \sin^2(\xi)}{\sqrt{2}}\Big(|0'1'\rangle - |1'0'\rangle\Big) = \frac{1}{\sqrt{2}}\Big(|0'1'\rangle - |1'0'\rangle\Big) = |\beta'_{11}\rangle\,. \tag{12}$$

The comparison of Eqs. (5), (6) with Eqs. (9), (12) reveals that the two entangled coding states $\big(|\beta_{00}\rangle , |\beta_{11}\rangle\big)$ can be considered as invariant when seen from a rotated basis $\{|0'\rangle , |1'\rangle\}$ at any angle $\xi$ in Eq. (2). When measuring separately the qubits of the pair by projecting in any rotated basis $\{|0'\rangle , |1'\rangle\}$, the state $|\beta_{00}\rangle$ of Eq. (9) always leads to two qubits found in the same state so as to decode a pixel value at 0, and the state $|\beta_{11}\rangle$ of Eq. (12) always leads to two qubits found in opposite states so as to decode a pixel value at 1. This recovers deterministically, with no error, the encoded pixel value, through measurements of two individual qubits in any rotated basis $\{|0'\rangle , |1'\rangle\}$. The

coding scheme especially no longer suffers from the detrimental effect, as illustrated in Fig. 1, of a rotation angle $\xi \neq 0$ between the coding and decoding bases.

Alternatively, instead of two separate measurements on each qubit, a (more elaborate) joint measurement of the qubit pair can be performed. When pixel coding is accomplished through the two entangled states $\left(|\beta_{00}\rangle\,, |\beta_{11}\rangle\right)$ defined via Eqs. (5)–(6) from the basis $\{|0\rangle\,, |1\rangle\}$ local to the coding stage, then decoding through a joint measurement of the qubit pair projecting in particular on the two entangled states $\left(|\beta'_{00}\rangle\,, |\beta'_{11}\rangle\right)$ defined via Eqs. (9), (12) from any rotated basis $\{|0'\rangle\,, |1'\rangle\}$ local to the decoding stage, leads in the same way to exact error-free decoding.

## 4 Decoding by measuring an observable on the qubit

When measuring a qubit with a two-outcome measurement, any statistics conceivable for the measurement outcomes can be obtained by measuring an observable $\Omega$ of the qubit under the form

$$\Omega = \boldsymbol{\omega} \cdot \boldsymbol{\sigma} = \omega_x \sigma_x + \omega_y \sigma_y + \omega_z \sigma_z \tag{13}$$

with $\boldsymbol{\omega} = [\omega_x, \omega_y, \omega_z]^\top$ a unit vector of $\mathbb{R}^3$, and $\boldsymbol{\sigma}$ a formal vector assembling the three $2 \times 2$ (traceless Hermitian unitary) Pauli matrices $[\sigma_x, \sigma_y, \sigma_z] = \boldsymbol{\sigma}$. The observable of Eq. (13) defines [18] a spin measurement in the direction $\boldsymbol{\omega}$ of $\mathbb{R}^3$.

Any qubit state of the complex two-dimensional Hilbert space $\mathcal{H}_2$ can be represented by a density operator $\rho$ on $\mathcal{H}_2$ expressible in Bloch representation as[18]

$$\rho = \frac{1}{2}\Big(\mathrm{I}_2 + \mathbf{r} \cdot \boldsymbol{\sigma}\Big), \tag{14}$$

with $\mathrm{I}_2$ the $2 \times 2$ identity matrix on $\mathcal{H}_2$, and a Bloch vector $\mathbf{r} = [r_x, r_y, r_z]^\top \in \mathbb{R}^3$ of unit Euclidean norm $\|\mathbf{r}\| = 1$ for a pure state, as considered here for image coding, and $\|\mathbf{r}\| < 1$ for a mixed state.

Any qubit observable $\Omega$ as in Eq. (13) has two eigenvalues $\omega_\pm = \pm 1$ which as measurement outcomes can be used to decode the two binary pixel values 0/1. The two associated eigenstates are $|\omega_\pm\rangle$ defined in Eq. (14) by the two Bloch vectors $\pm\boldsymbol{\omega}$. Measuring the observable $\Omega$ of Eq. (13) is equivalent to performing a projective measurement in its orthonormal eigenbasis expressible as

$$\begin{cases} |\omega_+\rangle = +\cos(\theta/2)\,|0\rangle + e^{i\varphi}\sin(\theta/2)\,|1\rangle \\ |\omega_-\rangle = -\sin(\theta/2)\,|0\rangle + e^{i\varphi}\cos(\theta/2)\,|1\rangle \end{cases} \tag{15}$$

associated with a Bloch vector under the form $\boldsymbol{\omega} = [\omega_x = \sin(\theta)\cos(\varphi), \omega_y = \sin(\theta)\sin(\varphi), \omega_z = \cos(\theta)]^\top$ which is the general form of a unit vector in $\mathbb{R}^3$ defined by a coelevation angle $\theta \in [0, \pi]$ with the $Oz$ axis and an azimuth angle $\varphi \in [0, 2\pi)$ around the $Oz$ axis.

The orthonormal basis $\{|\omega_+\rangle\,, |\omega_-\rangle\}$ of Eq. (15) used as a projective basis defines the most general two-outcome measurement for a qubit, characterized by two angles

$(\theta, \varphi)$ as degrees of freedom. By comparison, the projective basis $\{|0'\rangle, |1'\rangle\}$ of Eq. (2) represents a more restricted class of measurements, assuming $\varphi = 0$, and corresponding to observables $\Omega$ defined by $\boldsymbol{\omega} = [\omega_x = \sin(\theta), \omega_y = 0, \omega_z = \cos(\theta)]^\top$ lying in plane $(Ox, Oz)$ of $\mathbb{R}^3$ with a single angle $\xi = \theta/2$ as degree of freedom.

In this respect, the restricted class of decoding bases $\{|0'\rangle, |1'\rangle\}$ of Eq. (2) is appropriate to represent an arbitrary mismatch between the coding and decoding bases, only if the emitter and receiver share at least one common axis of reference. One common axis shared between the emitter and receiver allows the receiver to set up a measurement in a plane $(Ox, Oz)$ corresponding to an azimuth $\varphi = 0$. A shared common axis is therefore a necessary (and sufficient) condition to have access to the coding scheme of Sect. 3 allowing error-free decoding from any rotated basis $\{|0'\rangle, |1'\rangle\}$ of Eq. (2) through separate measurement of individual qubits. In particular, the rotation angle $\xi$ between the coding and decoding bases needs not be known and has no impact on the decoding, provided the emitter and receiver share a common axis to refer the rotation by the arbitrary (unknown) angle $\xi$.

In practice, the condition of a shared common axis represents a rather natural situation, which can be met relatively frequently. This is, for instance, the case each time a particle delivery link, such as a light beam, materializes a physical axis common to the emitter and receiver [13]. Sometimes also, the solid-state structure of quantum components establishes such a shared physical axis [13]. Also, the condition of frame alignment limited to a shared axis is investigated as a realistic and meaningful circumstance in various tasks of quantum communication, such as cryptographic key distribution [13] or entanglement assertion [15–17]. Beyond, we shall next demonstrate the possibility of an invariant image coding with strictly no alignment information (no common frame, no common axis) shared between the emitter and receiver.

## 5 Coding invariance with an arbitrary frame

With strictly no shared alignment information, the receiver refers the qubits to a local orthonormal basis $\{|0'\rangle, |1'\rangle\}$ related to the coding basis $\{|0\rangle, |1\rangle\}$ via an arbitrary unitary transform

$$\begin{cases} |0'\rangle = a\,|0\rangle + b\,|1\rangle \\ |1'\rangle = c\,|0\rangle + d\,|1\rangle \end{cases} \tag{16}$$

with complex coefficients $(a, b, c, d) \in \mathbb{C}^4$ yielding the unit-modulus determinant $|ad - bc| = 1$ by unitarity of Eq. (16). Also, both the rows and columns of the $2 \times 2$ unitary matrix $[a\ \ b; c\ \ d]$ defined by Eq. (16) form two sets of orthonormal vectors, implying the conditions $|a|^2 + |b|^2 = 1$, $|c|^2 + |d|^2 = 1$, $ac^* + bd^* = 0$, and $|a|^2 + |c|^2 = 1$, $|b|^2 + |d|^2 = 1$, $ab^* + cd^* = 0$. Equation (2) is a special case of Eq. (16) with real $(a, b, c, d) \in \mathbb{R}^4$; meanwhile, given all the constraints on $(a, b, c, d) \in \mathbb{C}^4$, Eq. (15) offers an equivalent general parametrization of the unitary transform of Eq. (16).

By using Eq. (16) for developing the tensor products for $|0'1'\rangle = |0'\rangle \otimes |1'\rangle$ and $|1'0'\rangle = |1'\rangle \otimes |0'\rangle$, it follows

$$|0'1'\rangle = ac\,|00\rangle + ad\,|01\rangle + bc\,|10\rangle + bd\,|11\rangle \tag{17}$$

$$|1'0'\rangle = ac\,|00\rangle + bc\,|01\rangle + ad\,|10\rangle + bd\,|11\rangle \tag{18}$$

and by summation of Eqs. (17) and (18),

$$|\beta'_{11}\rangle = \frac{1}{\sqrt{2}}\Big(|0'1'\rangle - |1'0'\rangle\Big) = (ad-bc)\frac{1}{\sqrt{2}}\Big(|01\rangle - |10\rangle\Big) = (ad-bc)\,|\beta_{11}\rangle \tag{19}$$

indicating that, up to an irrelevant global phase factor $ad - bc = e^{i\gamma}$, the Bell state $|\beta'_{11}\rangle$ of Eq. (19) local to the receiver, is equivalent to the analogue Bell state $|\beta_{11}\rangle$ of Eq. (6) local to the emitter. The entangled Bell state, or singlet state, $|\beta_{11}\rangle$ defined by Eq. (6) is therefore in this respect invariant in any unitary transform according to Eq. (16). The two one-dimensional subspaces of $\mathcal{H}_2 \otimes \mathcal{H}_2$ spanned, respectively, by $|\beta_{11}\rangle$ and by $|\beta'_{11}\rangle$ therefore coincide, i.e., $\text{span}\big(|\beta_{11}\rangle\big) \equiv \text{span}\big(|\beta'_{11}\rangle\big)$ is an invariant subspace through the transformation of Eq. (16).

It is now useful to introduce the two other Bell states[18]

$$|\beta_{01}\rangle = \frac{1}{\sqrt{2}}\Big(|01\rangle + |10\rangle\Big) \tag{20}$$

$$|\beta_{10}\rangle = \frac{1}{\sqrt{2}}\Big(|00\rangle - |11\rangle\Big) \tag{21}$$

which together with Eqs. (5)–(6) form the orthonormal Bell basis $\{|\beta_{00}\rangle, |\beta_{01}\rangle, |\beta_{10}\rangle, |\beta_{11}\rangle\}$ of $\mathcal{H}_2 \otimes \mathcal{H}_2$, in its version local to the emitter. There is also the analogously defined orthonormal Bell basis $\{|\beta'_{00}\rangle, |\beta'_{01}\rangle, |\beta'_{10}\rangle, |\beta'_{11}\rangle\}$ of $\mathcal{H}_2 \otimes \mathcal{H}_2$ referred to the computational basis $\{|0'\rangle, |1'\rangle\}$ local to the receiver. An important point is that each of these two Bell bases, local to the emitter and to the receiver, is an orthogonal basis of $\mathcal{H}_2 \otimes \mathcal{H}_2$. The three-dimensional subspace $\text{span}\big(|\beta_{00}\rangle, |\beta_{01}\rangle, |\beta_{10}\rangle\big)$ represents the (unique) orthogonal complement of $\text{span}\big(|\beta_{11}\rangle\big)$ in $\mathcal{H}_2 \otimes \mathcal{H}_2$. In the same way, the three-dimensional subspace $\text{span}\big(|\beta'_{00}\rangle, |\beta'_{01}\rangle, |\beta'_{10}\rangle\big)$ represents the (unique) orthogonal complement of $\text{span}\big(|\beta'_{11}\rangle\big)$ in $\mathcal{H}_2 \otimes \mathcal{H}_2$. Since $\text{span}\big(|\beta_{11}\rangle\big)$ and $\text{span}\big(|\beta'_{11}\rangle\big)$ coincide, and the unitary transform from Eq. (16) preserves orthogonality; therefore, $\text{span}\big(|\beta_{00}\rangle, |\beta_{01}\rangle, |\beta_{10}\rangle\big)$ and $\text{span}\big(|\beta'_{00}\rangle, |\beta'_{01}\rangle, |\beta'_{10}\rangle\big)$ also coincide and represent the same subspace of $\mathcal{H}_2 \otimes \mathcal{H}_2$ orthogonal to $\text{span}\big(|\beta_{11}\rangle\big) \equiv \text{span}\big(|\beta'_{11}\rangle\big)$. This means that, through the transformation of Eq. (16) relating the reference frames of the emitter and of the receiver, $\text{span}\big(|\beta_{00}\rangle, |\beta_{01}\rangle, |\beta_{10}\rangle\big) \equiv \text{span}\big(|\beta'_{00}\rangle, |\beta'_{01}\rangle, |\beta'_{10}\rangle\big)$ is an invariant subspace of $\mathcal{H}_2 \otimes \mathcal{H}_2$.

In this way, any state prepared in $\text{span}\big(|\beta_{00}\rangle, |\beta_{01}\rangle, |\beta_{10}\rangle\big)$ by the emitter is seen by the receiver in $\text{span}\big(|\beta'_{00}\rangle, |\beta'_{01}\rangle, |\beta'_{10}\rangle\big)$, for any transformation in Eq. (16) relating the emitter frame $\{|0\rangle, |1\rangle\}$ and the receiver frame $\{|0'\rangle, |1'\rangle\}$. This can especially be verified explicitly by direct computation (although this is now granted from our previous geometric argument) for the three Bell states $|\beta'_{00}\rangle$, $|\beta'_{01}\rangle$ and $|\beta'_{10}\rangle$, as it was accomplished for the Bell state $|\beta'_{11}\rangle$ with Eq. (19), through the use of Eqs. (17)–(18), now complemented from Eq. (16) by

$$|0'0'\rangle = a^2\,|00\rangle + ab\,|01\rangle + ab\,|10\rangle + b^2\,|11\rangle \tag{22}$$

$$|1'1'\rangle = c^2\,|00\rangle + cd\,|01\rangle + cd\,|10\rangle + d^2\,|11\rangle \tag{23}$$

and establishing these three states as linear combinations of $|\beta_{00}\rangle$, $|\beta_{01}\rangle$ and $|\beta_{10}\rangle$. For any unitary transform in Eq. (16), we therefore have two invariant orthogonal subspaces, $\text{span}\big(|\beta_{11}\rangle\big)$ and $\text{span}\big(|\beta_{00}\rangle\,,|\beta_{01}\rangle\,,|\beta_{10}\rangle\big)$, realizing a direct sum for $\mathcal{H}_2 \otimes \mathcal{H}_2$. This provides the ground for a coding scheme of binary images allowing frame-independent decoding.

For a frame-independent coding scheme of binary images, the pixel value 0 is, for instance, coded by the two-qubit state $|\beta_{00}\rangle$ of Eq. (5), and the pixel value 1 coded by the two-qubit state $|\beta_{11}\rangle$ of Eq. (6), (or conversely), relative to the local reference frame of the emitter. Then for binary decoding, the receiver sets up a two-outcome measurement acting jointly on the qubit pair, and formed by the two orthogonal projectors $(\Pi_0, \Pi_1)$ decomposing the identity $\mathrm{I}_4 = \mathrm{I}_2 \otimes \mathrm{I}_2 = \Pi_0 + \Pi_1$ of $\mathcal{H}_2 \otimes \mathcal{H}_2$. The projector $\Pi_0 = |\beta'_{00}\rangle\langle\beta'_{00}| + |\beta'_{01}\rangle\langle\beta'_{01}| + |\beta'_{10}\rangle\langle\beta'_{10}|$ projects on the invariant subspace $\text{span}\big(|\beta'_{00}\rangle\,,|\beta'_{01}\rangle\,,|\beta'_{10}\rangle\big) \equiv \text{span}\big(|\beta_{00}\rangle\,,|\beta_{01}\rangle\,,|\beta_{10}\rangle\big)$, while the projector $\Pi_1 = |\beta'_{11}\rangle\langle\beta'_{11}|$ projects on the invariant subspace $\text{span}\big(|\beta'_{11}\rangle\big) \equiv \text{span}\big(|\beta_{11}\rangle\big)$. In this way, in any reference frame local to the receiver, when the qubit pair upon measurement is projected in $\text{span}\big(|\beta'_{00}\rangle\,,|\beta'_{01}\rangle\,,|\beta'_{10}\rangle\big)$, this decodes the pixel value 0, and when it is projected in $\text{span}\big(|\beta'_{11}\rangle\big)$, this decodes the pixel value 1, so achieving exact error-free decoding. We note that any state in $\text{span}\big(|\beta_{00}\rangle\,,|\beta_{01}\rangle\,,|\beta_{10}\rangle\big)$ could be used as a coding state in place of $|\beta_{00}\rangle$ and would preserve an invariant coding. For instance, the same invariant coding is shown with $|00\rangle$ for transmitting one bit of classical information in [12] outside the field of image processing. However, the Bell state $|\beta_{00}\rangle$, or alternatively $|\beta_{01}\rangle$, is preferable for additional properties of resistance to noise or decoherence of the code, as we next show.

## 6 Resistance to noise

The invariant coding of Sect. 5 based on the two entangled two-qubit states $(|\beta_{00}\rangle\,,|\beta_{11}\rangle)$ also brings in some superior resistance to quantum noise or decoherence. With direct image coding with the two one-qubit states $(|0\rangle\,,|1\rangle)$ examined in Sect. 2, there is no frame invariance and also no immunity to the bit-flip noise of Eq. (4). In fact, both phenomena acting separately have an equivalent detrimental effect, as illustrated in Fig. 1, spoiling image decoding. Conversely, the coding based on $(|\beta_{00}\rangle\,,|\beta_{11}\rangle)$ in Sect. 5 displays general frame invariance and is also more resistant to bit-flip noise as we now show.

The action of the bit-flip noise on one qubit in $\mathcal{H}_2$, as defined by Eq. (4), can be extended to a qubit pair in $\mathcal{H}_2 \otimes \mathcal{H}_2$. Application of Eq. (4) to each qubit in the pair leads to the transformation for the two-qubit Bell states as follows:

$$\mathcal{N}\otimes\mathcal{N}\big(|\beta_{00}\rangle\langle\beta_{00}|\big) = \big[(1-p)^2+p^2\big]\,|\beta_{00}\rangle\langle\beta_{00}| + 2(1-p)p\,|\beta_{01}\rangle\langle\beta_{01}| \tag{24}$$

$$\mathcal{N}\otimes\mathcal{N}\big(|\beta_{01}\rangle\langle\beta_{01}|\big) = \big[(1-p)^2+p^2\big]\,|\beta_{01}\rangle\langle\beta_{01}| + 2(1-p)p\,|\beta_{00}\rangle\langle\beta_{00}| \tag{25}$$

$$\mathcal{N}\otimes\mathcal{N}\big(|\beta_{10}\rangle\langle\beta_{10}|\big) = \big[(1-p)^2+p^2\big]\,|\beta_{10}\rangle\langle\beta_{10}| + 2(1-p)p\,|\beta_{11}\rangle\langle\beta_{11}| \tag{26}$$

$$\mathcal{N}\otimes\mathcal{N}\left(|\beta_{11}\rangle\langle\beta_{11}|\right)=\left[(1-p)^2+p^2\right]|\beta_{11}\rangle\langle\beta_{11}|+2(1-p)p\,|\beta_{10}\rangle\langle\beta_{10}|\,. \quad (27)$$

From Eq. (24) it is seen that the coding state $|\beta_{00}\rangle$ through the action of the bit-flip noise always remains in the subspace $\text{span}\left(|\beta_{00}\rangle\,,|\beta_{01}\rangle\right)$, and a fortiori in the invariant subspace $\text{span}\left(|\beta_{00}\rangle\,,|\beta_{01}\rangle\,,|\beta_{10}\rangle\right)\equiv\text{span}\left(|\beta'_{00}\rangle\,,|\beta'_{01}\rangle\,,|\beta'_{10}\rangle\right)$; it will therefore always be decoded correctly, restoring the pixel value 0 with no error, for any probability $p$ characterizing the bit-flip noise. On the contrary, the coding state $|\beta_{11}\rangle$ through the action of the bit-flip noise in Eq. (27) is changed to the state $|\beta_{10}\rangle$ with probability $2(1-p)p$. In this circumstance, the decoding scheme will produce an error, by decoding incorrectly the pixel value 0 instead of the pixel value 1. Such decoding error occurs with the probability $2(1-p)p$ of measuring the qubit pair outside the invariant subspace $\text{span}\left(|\beta_{11}\rangle\right)\equiv\text{span}\left(|\beta_{11}\rangle\right)$. This probability of error $2(1-p)p$ is therefore invariant with the local frame used by the receiver for decoding. This coding–decoding process of a binary image, with one of the two coding states being completely immune to the noise, can be interpreted as a classical information channel known as a Z-channel [25].

For a classical Z-channel transmitting the symbol 0 with no error and the symbol 1 with a probability of error $q$, the input–output mutual information can be computed from the standard entropies and comes out as [25,26]

$$I_{\text{Z}}=h\big((1-q)P_1\big)+h\big(1-(1-q)P_1\big)-\big[h(q)+h(1-q)\big]P_1 \quad (28)$$

with the function $h(u)=-u\log_2(u)$ and $P_1$ the probability of a symbol 1 at the input. $I_{\text{Z}}$ is maximized by the input probability

$$P_1^*=\frac{q^{q/(1-q)}}{1+(1-q)q^{q/(1-q)}} \quad (29)$$

achieving capacity. In the presence of the bit-flip noise of Eq. (4) with flipping probability $p$, the frame-invariant coding–decoding based on $(|\beta_{00}\rangle\,,|\beta_{11}\rangle)$ realizes a classical Z-channel with probability of error $q=2(1-p)p$. Meanwhile, the direct coding–decoding with the states $(|0\rangle\,,|1\rangle)$ realizes a classical binary symmetric channel with bit error probability $p$, having an input–output mutual information also computable from the standard entropies [26] as

$$I_{\text{S}}=h\big(p(1-P_1)+(1-p)P_1\big)+h\big(pP_1+(1-p)(1-P_1)\big)-h(p)-h(1-p) \quad (30)$$

which is maximized for equiprobability of the two input symbols. A superior noise resistance between the two coding schemes is manifested, for any given flipping probability $p$ in Eq. (4), by a mutual information $I_{\text{Z}}(p)$ which is always above $I_{\text{S}}(p)$, as shown in the typical conditions of Fig. 2 at two values of the probability $P_1$.

To complement the typical illustrations of Fig. 2, due to the complicated nonlinear forms of Eqs. (28) and (30), it is difficult to obtain a formal proof of $I_{\text{Z}}\geq I_{\text{S}}$ for all relevant configurations of $(P_1,\,p)$. It is, however, straightforward to use Eqs. (28) and (30) for direct numerical computation of the difference $I_Z-I_S$. The relevant

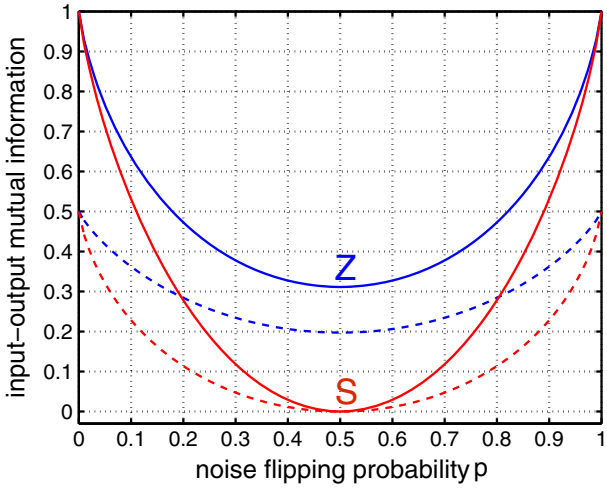


**Fig. 2** As a function of the flipping probability $p$ of the quantum bit-flip noise in Eq. (4), the input–output mutual information $I_Z$ of Eq. (28) (two *blue curves* marked Z) characterizing the frame-invariant coding–decoding based on $(|\beta_{00}\rangle, |\beta_{11}\rangle)$, and $I_S$ of Eq. (30) (two *red curves* marked S) characterizing the direct coding–decoding with $(|0\rangle, |1\rangle)$ with no frame invariance. In the binary image, the probability of a symbol 1 is $P_1 = 0.5$ (*solid lines*), and $P_1 = 0.11$ (*dashed lines*) (Color figure online)

domain is $(P_1, p) \in [0, 1/2] \times [0, 1]$ since one always has the option of selecting the noise-immune binary state of the Z-channel as the binary pixel value predominant in the input image. Over this domain, with a very fine grid for $(P_1, p)$ with step $10^{-4}$ in both directions, $I_Z - I_S$ was everywhere found nonnegative and smooth, providing strong numerical evidence suggesting $I_Z \geq I_S$ everywhere, as illustrated in Fig. 2.

Also in Fig. 2, over a wide range of $p$ around $1/2$, the mutual information $I_Z$ associated with a two-qubit per pixel (frame-invariant) code, is larger than twice $I_S$ associated with a one qubit per pixel (non-frame-invariant) code. So per qubit, the frame-invariant code keeps also a significant superiority over the non-frame-invariant code.

For another illustration of the superior noise resistance of the frame-invariant scheme of Sect. 5, Fig. 3 displays the behavior of the frame-invariant coding of the binary image of Fig. 1 when affected by the quantum bit-flip noise of Eq. (4) at different values of the flipping probability $p$. The binary image involved in Figs. 1 and 3 has a fraction 0.89 of white pixels; accordingly, the white pixels (predominant) are coded by the quantum state $|\beta_{00}\rangle$ associated with a decoding immune to the noise, and corresponding to a probability $P_1 = 0.11$ as in Fig. 2.

The four noise conditions (four values of $p$) illustrated in Fig. 3 are quantitatively characterized in Fig. 2 by the input–output mutual information $I_Z$ at $P_1 = 0.11$ and the corresponding values of $p$ in abscissa. Also quantitatively for Fig. 3, the frame-invariant coding allows a probability of 1 for a white pixel at the input to be decoded as a white pixel at the output (noise immunity), and a probability of $q = 2(1-p)p$ for a black pixel at the input to be decoded as a white pixel at the output (noise error), these

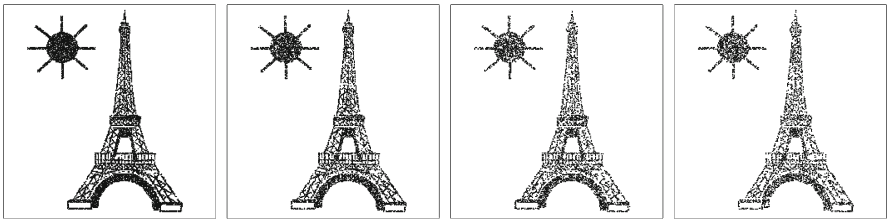

**Fig. 3** An original binary image (the *leftmost* image of Fig. 1) coded by the frame-invariant scheme based on $(|\beta_{00}\rangle, |\beta_{11}\rangle)$ for *white/black* pixels, then corrupted by the bit-flip noise of Eq. (4) with flipping probability $p$, and finally decoded as in Sect. 5. From *left* to *right* $p = 0.095$, 0.206, 0.345 and 0.5, equivalent via $p = \sin^2(\xi)$ to the effect of a mismatch angle $\xi$ at the same values $\xi = 0.1\pi$, $0.15\pi$, $0.2\pi$ and $0.25\pi$ of Fig. 1

two probabilities being combined to determine the input–output mutual information $I_Z$ in Fig. 2.

By comparing Figs. 3 and 1 at similar levels of $p$ (or $\xi$) assessing the degradation, visual perception also manifests the superior quality of the images of Fig. 3 benefiting from the frame-invariant coding of Sect. 5, and especially the noise immunity it can confer to the predominant class of (white) pixels. At the most detrimental flipping probability $p = 0.5$ (or $\xi = 0.25\pi$) of the noise, the corresponding binary image in Fig. 1 has become completely random, in accordance with the mutual information $I_S(p = 0.5) = 0$ in Fig. 2 at $P_1 = 0.11$. Meanwhile, at this $p = 0.5$, the comparable binary image in Fig. 3 keeps significant similarity with the original noise-free image, in accordance with the mutual information $I_Z(p = 0.5) \approx 0.2$ strictly above zero in Fig. 2 at $P_1 = 0.11$. For complementing the Shannon mutual information of Fig. 2 and the visual appreciation of Fig. 3, other quantitative generalized information metrics [27,28] could also be used for other viewpoints on the enhanced resistance to noise of the invariant coding.

## 7 Conclusion

In this paper, we considered quantum coding of binary images. Non-binary images, such as gray images, with pixel intensities represented on an arbitrary number of bits (typically 8, 12 or 16) are also concerned by considering each of their bit planes as a binary image. And color images with their three red, green and blue planes are also concerned by considering each of their three color planes as a gray image. We investigated the issue of a quantum coding performed by an emitter which would be decodable by a receiver in the absence of reference frames shared between the emitter and receiver. Direct coding with one qubit per pixel and no aligned frames leads to decoding errors equivalent to a quantum bit-flip noise having a level increasing with the misalignment between the coding and decoding frames. Consequently, instead of a coding scheme tied to an absolute reference frame, we turned to the possibility of a more relative coding leaning on the relative orientations of two qubits inside an entangled pair. We showed the feasibility of frame-invariant image coding by using for each pixel a qubit pair selectively prepared in the entangled Bell states $|\beta_{00}\rangle$ or $|\beta_{11}\rangle$

of Eqs. (5)–(6). Provided there is just one common axis shared between the emitter and receiver, we established that exact decoding for each pixel can be performed, by means of a two-outcome projective measurement in any orthonormal basis local to the receiver and operating separately on each qubit of the pair. Furthermore, in the more stringent condition where strictly no alignment information is shared between the emitter and receiver, we established that exact decoding can be performed, by measuring with two orthogonal projectors operating jointly on the qubit pair and projecting on two invariant subspaces realizing a direct sum of $\mathcal{H}_2 \otimes \mathcal{H}_2$. Projective quantum measurements are used here to realize the frame-invariant decoding restoring a classical image from its quantum representation. Such projective measurements of qubits are in principle very basic measurements, which are very often employed in quantum information and quantum communication. Their physical implementation will, however, depend on the physical realization of the qubit itself, for instance, with photon polarization, or electron spin, or otherwise [18,29,30].

In addition, we showed that the frame-invariant coding is much more resistant to quantum bit-flip noise compared to the direct non-invariant coding. So, for a cost per pixel of two (entangled) qubits instead of one, we obtain in this way complete frame invariance for image coding and enhanced noise resistance. The present invariant coding may also possibly be combined with other types of coding for quantum images [2–9,11], so as to add frame independence to other desirable properties of the coding. Also, as a bit-based method, the frame-invariant coding can be applied to any kind of bit-based quantum signal transmission, like audio signals for example.

The quantum bit-flip noise considered here arises naturally with binary images and their (misaligned) measurement as seen in Sect. 2. However, other quantum noises, such as phase-flip noise or depolarizing noise [18], could also be considered so as to assess their impact on the frame-independent coding developed here for images. The present coding scheme offers the option to select one of the two coding states in the invariant subspace span$\big(|\beta_{00}\rangle\,,|\beta_{01}\rangle\,,|\beta_{10}\rangle\big)$. This represents a relatively broad flexibility in the choice. Here with the bit-flip noise acting according to Eqs. (24)–(27), no choice can perform better than $|\beta_{00}\rangle$, which is completely immune to the noise. But with other noises, the choice of this coding state could be settled so as to optimize the decoding for maximally efficient detection or estimation from noisy qubits in the presence of definite quantum noises [31–33].

At the decoding stage, instead of performing quantum measurements to restore a classical binary image, it can be envisaged as an alternative to set up quantum circuits operating on the coded quantum states available at the receiver, so as to generate another quantum image under a form possibly more suitable to efficient processing by quantum algorithms. The initial quantum image will have benefited from the frame-independent coding for transmission, and at the receiving end it can then undergo lossless quantum recoding for local quantum processing. Efficient quantum image representations may in this respect turn out to be distinct for distinct informational operations, such as invariant transmission, resistance to noise, computing, or else. We have concentrated here on quantum image coding endowed with a frame-invariance property. This step can be pipelined with other steps of the image processing chain. One can, for instance, envision compression/decompression, denoising, enhancement,

segmentation and pattern recognition. In this way, our proposal of frame-invariant coding fits into the ongoing development of quantum image processing.

## References


1. Venegas-Andraca, S.E.: Introductory words: special issue on quantum image processing published by Quantum Information Processing. Quantum Inf. Process. **14**, 1535–1537 (2015)
2. Venegas-Andraca, S.E., Ball, J.L.: Processing images in entangled quantum systems. Quantum Inf. Process. **9**, 1–11 (2010)
3. Le, P.H., Dong, F., Hirota, K.: A flexible representation of quantum images for polynomial preparation, image compression, and processing operations. Quantum Inf. Process. **10**, 63–84 (2011)
4. Zhang, Y., Lu, K., Gao, Y., Wang, M.: NEQR: A novel enhanced quantum representation of digital images. Quantum Inf. Process. **12**, 2833–2860 (2013)
5. Li, H.-S., Qingxin, Z., Lan, S., Shen, C.-Y., Zhou, R., Mo, J.: Image storage, retrieval, compression and segmentation in a quantum system. Quantum Inf. Process. **12**, 2269–2290 (2013)
6. Li, H.-S., Zhu, Q., Zhou, R.-G., Li, M.-C., Song, I., Ian, H.: Multidimensional color image storage, retrieval, and compression based on quantum amplitudes and phases. Inf. Sci. **273**, 212–232 (2014)
7. Jobay, R., Sleit, A.: Quantum inspired shape representation for content based image retrieval. J. Signal Inf. Process. **5**, 54–62 (2014)
8. Caraiman, S., Manta, V.I.: Histogram-based segmentation of quantum images. Theor. Comput. Sci. **529**, 46–60 (2014)
9. Jiang, N., Wu, W., Wang, L., Zhao, N.: Quantum image pseudocolor coding based on the density-stratified method. Quantum Inf. Process. **14**, 1735–1755 (2015)
10. Mastriani, M.: Quantum Boolean image denoising. Quantum Inf. Process. **14**, 1647–1673 (2015)
11. Yan, F., Iliyasu, A.M., Venegas-Andraca, S.E.: A survey of quantum image representations. Quantum Inf. Process. **15**, 1–35 (2016)
12. Bartlett, S.D., Rudolph, T., Spekkens, R.W.: Reference frames, superselection rules, and quantum information. Rev. Mod. Phys. **79**, 555–610 (2007)
13. Laing, A., Scarani, V., Rarity, J.G., O'Brien, J.L.: Reference-frame-independent quantum key distribution. Phys. Rev. A **82**, 1–5 (2010). pp. 012304
14. Wallman, J.J., Bartlett, S.D.: Observers can always generate nonlocal correlations without aligning measurements by covering all their bases. Phys. Rev. A **85**, 1–4 (2012). pp. 024101
15. Shadbolt, P., Vértesi, T., Liang, Y.C., Branciard, C., Brunner, N., O'Brien, J.L.: Guaranteed violation of a Bell inequality without aligned reference frames or calibrated devices. Sci. Rep. **2**, 1–7 (2012). pp. 470
16. Lawson, T., Pappa, A., Bourdoncle, B., Kerenidis, I., Markham, D., Diamanti, E.: Reliable experimental quantification of bipartite entanglement without reference frames. Phys. Rev. A **90**, 1–7 (2014). pp. 042336
17. Senel, C.F., Lawson, T., Kaplan, M., Markham, D., Diamanti, E.: Demonstrating genuine multipartite entanglement and nonseparability without shared reference frames. Phys. Rev. A **91**, 1–6 (2015). pp. 052118
18. Nielsen, M.A., Chuang, I.L.: Quantum Computation and Quantum Information. Cambridge University Press, Cambridge (2000)
19. Rudolph, T., Grover, L.: Quantum communication complexity of establishing a shared reference frame. Phys. Rev. Lett. **91**, 1–4 (2003). pp. 217905
20. Peres, A., Scudo, P.F.: Transmission of a Cartesian frame by a quantum system. Phys. Rev. Lett. **87**, 1–4 (2001). pp. 167901
21. Bagan, E., Baig, M., Muñoz-Tapia, R.: Entanglement-assisted alignment of reference frames using a dense covariant coding. Phys. Rev. A **69**, 1–4 (2004). pp. 050303(R)
22. Bagan, E., Baig, M., Muñoz-Tapia, R.: Quantum reverse engineering and reference-frame alignment without nonlocal correlations. Phys. Rev. A **70**, 1–4 (2004). pp. 030301(R)
23. Chiribella, G., DAriano, G.M., Perinotti, P., Sacchi, M.F.: Efficient use of quantum resources for the transmission of a reference frame. Phys. Rev. Lett. **93**, 1–4 (2004). pp. 180503
24. Bahder, T.B.: Transfer of spatial reference frame using singlet states and classical communication. Quantum Inf. Process. **15**, 1069–1080 (2016)
25. Golomb, S.W.: The limit behavior of the Z-channel. IEEE Trans. Inf. Theory **26**, 372 (1980)

26. Cover, T.M., Thomas, J.A.: Elements of Information Theory. Wiley, New York (1991)
27. Chapeau-Blondeau, F., Rousseau, D., Delahaies, A.: Rényi entropy measure of noise-aided information transmission in a binary channel. Phys. Rev. E **81**, 1–10 (2010). pp. 051112
28. Chapeau-Blondeau, F.: Tsallis entropy for assessing quantum correlation with Bell-type inequalities in EPR experiment. Phys. A **414**, 204–215 (2014)
29. Everitt, H.: Special issue on experimental aspects of quantum computing: Introduction. Quantum Inf. Process. **3**, 1–4 (2004)
30. Jones, J.A., Jaksch, D.: Quantum Information, Computation and Communication. Cambridge University Press, Cambridge (2012)
31. Helstrom, C.W.: Quantum Detection and Estimation Theory. Academic Press, New York (1976)
32. Chapeau-Blondeau, F.: Optimization of quantum states for signaling across an arbitrary qubit noise channel with minimum-error detection. IEEE Trans. Inf. Theory **61**, 4500–4510 (2015)
33. Chapeau-Blondeau, F.: Optimized probing states for qubit phase estimation with general quantum noise. Phys. Rev. A **91**, 1–13 (2015). pp. 052310